

1 **Testing the validity of regional detail in global analyses of Sea**
2 **surface temperature — the case of Chinese coastal waters**

3 Yan Li^{1*}, Hans von Storch^{2,3}, Qinggyuan Wang⁴, Qingliang Zhou⁵, Shengquan Tang^{2,3}

4 ¹National Marine Data and Information Service, Tianjin, People's Republic of China

5 ²Institut für Küstenforschung, Helmholtz Zentrum Geesthacht, Germany

6 ³Ocean University of China, Qingdao, People's Republic of China

7 ⁴Tianjin Meteorological Observatory, Tianjin, People's Republic of China

8 ⁵Chinese Meteorological Administration, Beijing, People's Republic of China

9

10 **Abstract.** We have designed a method for testing the quality of multidecadal analyses of SST
11 in regional seas by using a set of high-quality local SST observations. In recognizing that
12 local data may reflect local effects, we focus on dominant EOFs of the local data and of the
13 localized data of the gridded SST analyses. We examine the patterns, variability as well as
14 trends of the principal components. This method is applied to examine three different SST
15 analyses, i.e., HadISST1, ERSST and COBE SST. They have been assessed using a newly
16 constructed high-quality data set of SST at 26 coastal stations along the Chinese coast in
17 1960–2015 which underwent careful examination with respect to quality, and a number of
18 corrections of inhomogeneities. The three gridded analyses perform by and large well from
19 1960 to 2015, in particular since 1980. However, for the pre-satellite period, prior to 1980s,
20 the analyses differ among each other and show some inconsistencies with the local data, such
21 as artificial break points, periods of bias and differences in trends. We conclude that gridded
22 SST-analyses need improvement in the pre-satellite period (prior to 1980s), by re-examining
23 in detail archives of local quality-controlled SST data in many data-sparse regions of the
24 world.

25

* Corresponding author. E-mail address: ly_nmdis@163.com

26 **1. Introduction**

27 Sea surface temperature (SST) is a key parameter for climate change assessments. It is
28 significantly associated with many atmospheric and oceanographic modes, such as Pacific
29 Decadal Oscillation (PDO), El Niño/South Oscillation (ENSO), Indian Ocean Dipole (IOD),
30 etc. (Saji et al., 1999, Mantua and Hare, 2002, Yeh and Kim, 2010). Long-term historical SST
31 data sets have been extensively used as a source of information on global and regional SST
32 trends and variability (Belkin, 2009; Wu et al., 2012; Boehme et al.2014; Hirahara et al.2014;
33 Stramska and Bialogrodzka, 2015). However, historical SST datasets have large uncertainties
34 in long-term trend patterns in some regions. For example, observed SST changes in the
35 tropical Pacific are still controversial, depending on the choice of the dataset and study period
36 (Bunge & Clarke 2009). Vecchiga et al. (2008) indicated that the equatorial zonal SST
37 gradient in the Pacific has intensified in Hadley Centre Sea Ice and Sea Surface Temperature
38 (HadISST) but weakened in Extended Reconstructed SST (ERSST) from the nineteenth to
39 twentieth centuries. Scientists utilized several different datasets, including the reconstructed
40 and un-interpolated datasets, to study the SST variability in tropical areas and the China Seas
41 (Xie et al., 2010; Liu and Zhang 2013, Tokinaga et al., 2012). They found that there were
42 large uncertainties in estimate of SST warming patterns using different SST datasets. Thus, it
43 is also necessary for comparing different SST products over the regional areas in detail.

44 Coastal marine ecosystems yield nearly half of the earth's total ecosystem goods and services
45 (Costanza, 1997). A study of SST changes in the world ocean with large marine ecosystems
46 revealed that the Subarctic Gyre, European Seas, and East Asian Seas warmed at rates 2–4
47 times the global mean rate (Belkin 2009). Recently, Lima and Wethey 2012 using a SST
48 dataset with higher spatial-temporal resolution detected that during the last three decades ~
49 71.6% of the world coastal locations have experienced a warming trend of 0.25 ± 0.13 °C per
50 decade and 6.8% a cooling of -0.11 ± 0.10 °C per decade. Increase in SST is especially
51 important in coastal areas due to its strong impact in coastal ecosystems (Honkoop et al., 1998;
52 Burrow et al., 2011; Wernberg et al. 2016). Simultaneously, coastal SST is highly influenced
53 by local factors, such as the anthropogenic land-based processes, upwelling currents, fresh
54 water discharge, ocean fronts and local tidal mixing. An accurate analysis of the local SST
55 and its variability is needed for marine ecosystem-based management. Here, we mainly focus
56 on three globally gridded SST datasets, that is, the HadISST1, ERSST, COBE SST (Rayner et
57 al., 2003, Ishii et al., 2005, Smith et al., 2008, Hirahara et al., 2014; Huang et al., 2015).
58 Besides, a fourth SST product is considered, i.e., NOAA Optimum Interpolation SST (OISST)

59 version 2 using Advanced Very High Resolution Radiometer infrared satellite SST data from
60 the Pathfinder satellite combined with buoy data, ship data, and sea ice data, covering from
61 1982 to present. Because of its high spatial resolution of $0.25^{\circ} \times 0.25^{\circ}$, it is used in the
62 concluding section for clarifying some additional aspect. All of these datasets have been
63 widely used in the regional and global climate change studies. Given that these datasets have
64 been developed by independent groups, there are some differences of data sources, bias
65 adjustment and reconstruction method, etc. in the SST analyses products. For example, some
66 analyses only use in situ observations, such as ERSST v4 and COBE SST. Others use both in
67 situ and satellite observations, such as OISST and HadISST1. There are also some differences
68 from quality control and gap-filling choices when and where observations are sparse,
69 particularly in early record periods and coastal areas (Huang et al., 2015; Li et al., 2017).
70 These differences also indicate some uncertainties in these SST analyses. In order to test the
71 validity of these gridded SST datasets along the coast of China, SST records for the period of
72 1960–2015 at total 26 Chinese coastal hydrological stations coast are used. All of these *in situ*
73 SST data from 1960 to 2015 are provided by the National Marine Data and Information
74 Service (NMDIS) of China and have been quality controlled and homogenized by Li et al.
75 (2018). These SST data from coastal hydrological stations have never been merged into
76 HadISST, COBE SST or other gridded SST analyses. Therefore, the homogenized long-term
77 SST observations along the Chinese coast can be used for evaluation on these analyses. We
78 study the performance of these gridded SST datasets in the coastal waters by comparing to the
79 homogenized SST.

80 Thus, the remainder of this paper is structured as follows: Details on the observational and
81 gridded data sets and methodology used in this study are given in section 2. Section 3
82 introduces the local homogenized SST series along the Chinese coast (Li et al., 2018), which
83 is used as a reference to compare to the gridded data sets with. For adding confidence in the
84 quality of this local SST data set, these SST data are compared with an independently
85 constructed local air temperature data. The basic statistics of the local SST-data series are also
86 shown. Section 4 describes the results and comparisons with gridded SST data sets in the
87 Chinese coastal waters. Further discussion and conclusion are given in section 5.

88 **2. Data and methodology**

89 **2.1. Data source**

90 The SST records during 1960–2015 at the 26 sites of coastal hydrological stations along the
91 Chinese coast have been assembled and homogenized. Homogenized monthly mean surface

92 air temperature (SAT) series from National Meteorological Information Center (NMIC) of
 93 China (Xu et al., 2013) and the gridded SAT from the latest version of the Climate Research
 94 Unit's (CRU) gridded high resolution (0.5°×0.5°) dataset CRU TS 3.24.01 for 1960–2015
 95 (Harris et al., 2014) are used to investigate the consistency of homogenized SST data with the
 96 local SAT.

97 Four globally gridded SST datasets are used in our work (see Table 1): (1) The 1°×1° Hadley
 98 Center Sea Ice and Sea Surface Temperature monthly dataset (HadISST) (Rayner et al., 2003);
 99 (2) The 1°×1° Centennial In Situ Observation-Based Estimates of the Variability of SST
 100 (COBE SST) (Hirahara et al., 2014); (3) 2°×2° Extended Reconstructed Sea Surface
 101 Temperature version 4 (ERSST v4) for 1960–2015 (Smith et al., 2008, Huang et al., 2015). (4)
 102 NOAA OISST v2 for 1982–2015 (Reynolds et al. 2007).

103 **Table 1.** Global gridded SST datasets that are used in this study

Dataset	Resolution	Period	Sources
ERSST v4	2°x 2°	1960– 2015	http://www.ncdc.noaa.gov/oa/climate/research/sst/ERSST.v4.php
HadISST	1°x 1°	1960– 2015	http://www.metoffice.gov.uk/hadobs/hadisst/data/download.html
COBE SST	1°x 1°	1960– 2015	http://ds.data.jma.go.jp/tcc/tcc/products/elnino/cobesst/cobe-sst.html
OISST	$\frac{1}{4} \circ \times \frac{1}{4} \circ$	1982– 2015	http://www.ncdc.noaa.gov/oisst

104 2.2. Methodology

105 Statistical methods such as conventional empirical orthogonal function (EOF) (Kim et al.,
 106 1996, von Storch and Zwiers 1999), correlation analysis and linear trend analysis are
 107 employed. The significance of each trend has been tested by the Mann-Kendall test using
 108 Sen's slope estimates quantify trends (Sen, 1968). The tests were stipulated to operate with a
 109 probability for a false rejection of the null hypotheses (i.e., zero trend) of 5%. They are
 110 conducted with the implicit assumption that the data are serially independent. There are only
 111 weakly correlated but not really independent. Thus, the tests are “liberal”, i.e., have
 112 tendencies for falsely rejecting too often the null hypothesis, when it is actually valid (von
 113 Storch and Zwiers, 1999). However, since the effect is relatively weak, given the small serial
 114 correlations, and since we have no results, which are close to the stipulated critical levels, we

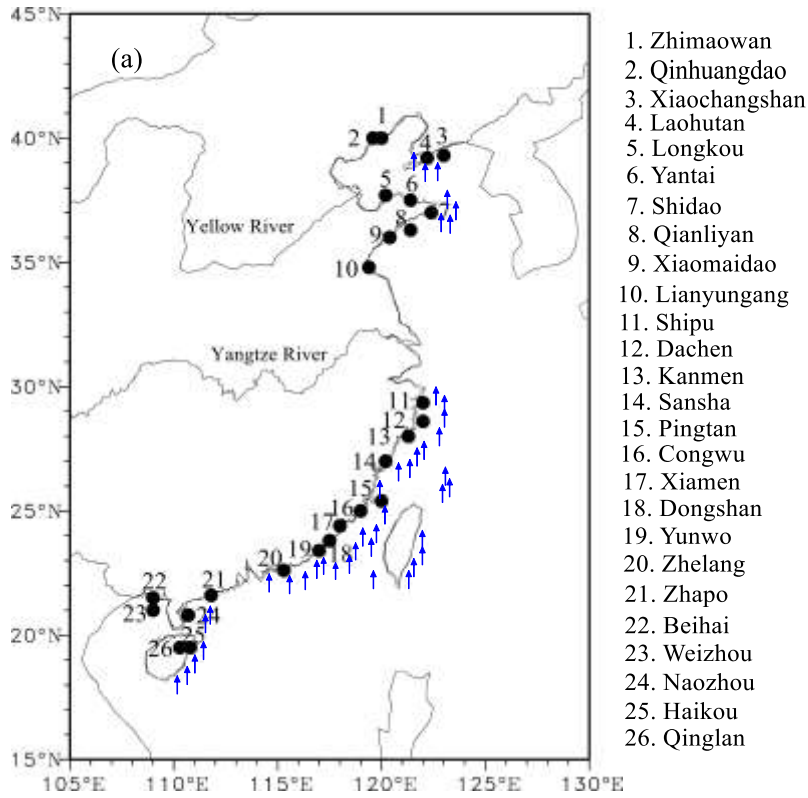
115 do as if the serial dependence is not of importance. However, this caveat should be kept in
116 mind, when assessing the results.

117 **3. The local homogenized SST records along the Chinese coast**

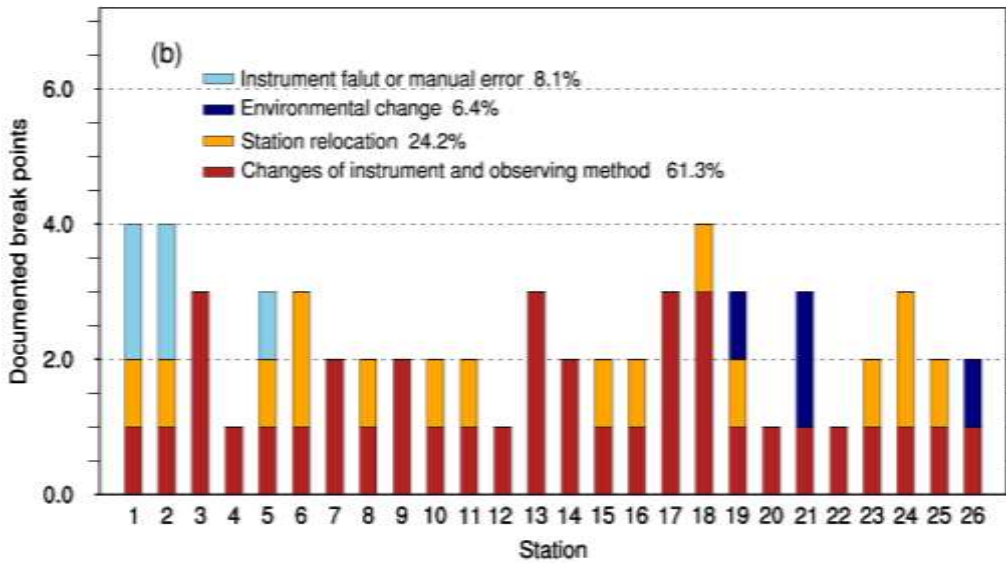
118 Currently, more than 100 coastal hydrological stations are operating and monitoring near-
119 shore hydrological conditions. Among these stations, only 26 stations have routinely and
120 continuously recorded since 1960, with a percentage of missing data less than 4%. Also, these
121 stations have undergone only a few (five or less) documented relocations. The locations of the
122 26 coastal hydrological stations are shown in Fig.1a. Monthly mean SST series were then
123 derived and subjected to a statistical homogeneity test, called the Penalized Maximum T
124 (PMT) test (more details can be found in Li et al., 2018). Homogenized monthly mean SST
125 series were obtained by adjusting all significant change points which were supported by
126 historic metadata information. These identified change points at each station are displayed in
127 Fig.1b. The majority of change points are caused by instrument changes and station
128 relocations, accounting for 60.6% and 24.6% of the total, respectively. In our work, we
129 consider annual mean values. Some analyses with seasonal mean values are also calculated,
130 but these are not covered by our present account and merely summarized. The supporting
131 evidences are provided by the Supplementary Online Material (SOM) in Appendix B.

132 The standard statistics derived from the data in the period of 1960–2015, that is, long-term
133 mean, the standard deviation of annual means and the decadal trends are listed in Table 2.
134 SSTs vary along the Chinese coast, between about 11.5 °C at the north and 25 °C at the
135 southernmost locations. The standard deviations are of the order of 0.50 °C at all locations,
136 with a maximum of 0.71 °C and a minimum of 0.43 °C. The decadal trends vary between 0.13
137 °C per decade to 0.29 °C per decade. Table 2 also provides the long-term means of the
138 homogenized data and of the raw (unhomogenized) data. The differences between the
139 homogenized data and the raw data (last column) vary between -2.26 K and 0.53 K. At 22 of
140 the 26 stations, a downward correction of the mean has been found necessary – only at Station
141 15 (Pingtan) and Station 23 (Weizhou) an upward change was stipulated, and in two case
142 nearly no change of the mean at Station 7 (Shidao) and Station 24 (Naozhou).

143



144



145

146 **Figure 1.** Study area and locations of 26 coastal sites (a), for which continuous monthly SST recordings are
 147 available and corrected by eliminating inhomogeneities. The number of identified breakpoints in individual
 148 SST stations from 1960–2015 (b). Result from Li et al. (2018). Black circle represents 26 coastal sites and
 149 blue arrow represents coastal upwelling.

150

151 **Table 2.** Statistics of the time series of the annual homogenized local SST, plus the differences to the raw
 152 data, which were used to construct the homogenized series (columns 6 and 7).

Station No.	Full name	Mean homogenized SST	Standard deviation	Trend (°C/10yrs)	Mean unhomogenized SST	Diff
-------------	-----------	----------------------	--------------------	------------------	------------------------	------

1	Zhimaowan	11.50	0.53	0.17	11.75	-0.25
2	Qinhuangdao	12.21	0.59	0.26	12.32	-0.11
3	Xiaochangshan	11.54	0.71	0.29	11.73	-0.19
4	Laohutan	11.36	0.59	0.21	11.47	-0.11
5	Longkou	13.36	0.59	0.22	13.51	-0.15
6	Yantai	12.65	0.59	0.17	12.79	-0.14
7	Shidao	12.09	0.59	0.14	12.08	0.01
8	Qianliyan	14.37	0.65	0.17	14.41	-0.04
9	Xiaomaidao	13.76	0.63	0.22	13.84	-0.08
10	Lianyungang	14.85	0.57	0.21	14.94	-0.08
11	Shipu	17.41	0.65	0.26	18.01	-0.61
12	Dachen	17.67	0.65	0.24	17.91	-0.24
13	Kanmen	18.20	0.56	0.17	18.42	-0.22
14	Sansha	19.21	0.71	0.21	19.91	-0.19
15	Pingtang	19.72	0.61	0.19	19.45	0.53
16	Congwu	19.98	0.52	0.17	22.18	-0.64
17	Xiamen	21.50	0.51	0.19	21.47	-2.26
18	Dongshan	20.84	0.45	0.13	21.12	-0.28
19	Yunwo	21.02	0.44	0.13	21.36	-0.34
20	Zhelang	22.43	0.44	0.15	22.62	-0.19
21	Zhapo	23.62	0.50	0.18	23.68	-0.06
22	Beihai	23.60	0.55	0.18	24.06	-0.46
23	Weizhou	25.79	0.43	0.17	25.66	0.13
24	Naozhou	24.46	0.49	0.16	24.44	0.02
25	Haikou	25.00	0.49	0.16	25.10	-0.10
26	Qinglan	25.80	0.44	0.18	25.86	-0.07

153

154 The quality of the data set has already been documented by Li et al. (2018). To add
155 confidence in the quality of this data set, we compared the new data set to an independent data
156 set of local SAT at 26 nearby local stations. Also, this data set has been homogenized –
157 independently of the processing of the SST series. SST and SAT data are not compares
158 directly pairwise, but in terms of the patterns and coefficient time series (PCs) of their EOFs.
159 The similarity of the principal components is striking. The first PCs share a correlation
160 coefficient of 0.97, and the second 0.86 (Fig.A1). Thus, the SST series are fully consistent
161 with these SAT series. When this exercise is repeated with CRU TS 3.24.01 instead of the in-
162 situ SAT series, we find a similar consistency (see Fig. SOM-1). The PCs of SAT-CRU also
163 show high correlations of 0.94 and 0.83 with the in situ SST (see Fig. SOM-1) (more details

164 are shown in Appendix A and B). Thus, we conclude that our homogenized SST data is
165 superior to earlier used data on the SST variability and trends along the Chinese coast.

166 **4. Comparison with gridded SST datasets in the Chinese coast waters**

167 Given the consistency of the newly homogenized SST series with independent regional SAT
168 data, we use it as a benchmark for assessing the regional quality of the four globally gridded
169 SST data sets in Table 1. In the following, we name the new data set “Local homogenized
170 SST” as “LH”, while the datasets extracted from the gridded SST datasets as “localized
171 analysis data”, and use the abbreviation “LA”. For instance, LA-HadISST is the SST found in
172 HadISST in the local grid box, which contains the locations in the LH data set.

173 These “localized” time series (LA) of the three gridded datasets, which extend to the full time
174 window 1960–2015 (ERSST, HadISST, COBE SST; referred as LA-ERSST, LA-HadISST,
175 LA-COBE SST) are then compared to the local series — LH, by first comparing the standard
176 deviations and the trends, and by calculating from trends, differences (Diff) and the root mean
177 square errors (RMSEs) for the 26 stations (Table 3). We do this for annual mean values. The
178 fourth dataset, OISST data, covers a shorter time window from 1982–2015 and has a high
179 spatial resolution. It is used in the concluding section for clarifying some additional aspects in
180 the section 5.

181 For summarizing the results, we compute EOFs of the LH and the LAs, as well as for the
182 differences of LH and LAs. The LH data are derived from observational stations, whereas the
183 LA data are representing area values averaged across a grid box. Therefore, the LA data
184 should vary less than the LH data. Possible mismatches between the local LH data and the
185 spatial averages of grid box data in the LAs may be related to small scale effects; however,
186 the usage of EOFs is expected to reduce these truly local specifics, as the first EOFs describe
187 joint co-variations among the 26 elements in both LA and LH data sets.

188 **4.1. Comparing with HadISST**

189 The 56-year mean values of local SST in the analysis LA-HadISST are in all cases higher than
190 at the local stations (Table 3). Some differences are of the order of 2K and even 3K, in
191 particular along the East China Sea extending from Station 11 (Shipu) to Station 20 (Zhelang).
192 To some extent, this difference may reflect differences between averages of a larger coastal
193 ocean area and *in situ* observations, but not entirely.

194 The variations in LA are similar to LH, but there are some differences: as expected, 65.4% of
 195 the standard deviations (17) are larger for LH, and 34.6% cases (9) smaller. The correlations
 196 are all large enough to reject the null hypothesis of the absence of a link (if we assume serially
 197 independence the 90%-critical value is 0.22) except for the northernmost Station 19 (Yunwo).
 198 Part of the difference to the ideal value of 1 may be due to the different spatial scale, but
 199 values as low as 0.41 indicate to more systematic differences. The trends are positive for all
 200 sites (Table 3) – only the northernmost Station 1 (Zhimaowan) signals a weak downward
 201 trend in the LA-HadISST data set. In about 50% of the case, the coastal sea warms faster
 202 according to LH than to LA-HadISST, and for 50% it is the opposite. For the two
 203 northernmost sites, Station 1 (Zhimaowan) and Station 2 (Qinhuangdao), the warming
 204 according to LA is very weak, whereas along the stretch from Station 15 (Pingtan) to Station
 205 19 (Yunwo) the warming according to LA-HadISST is considerably stronger than in LH.

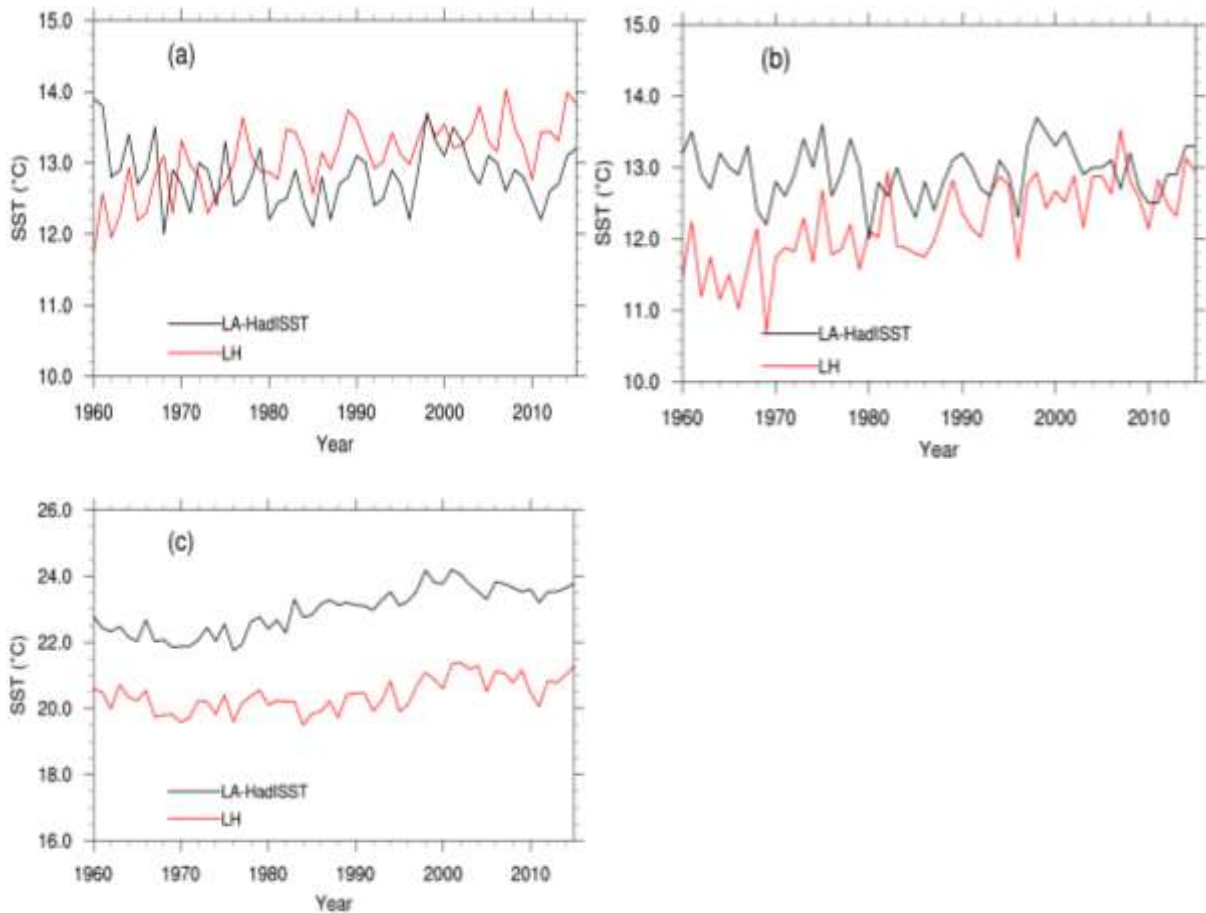
206 The time series for the two northern sites in the Bohai Sea are shown in Fig. 2. The sequence
 207 of maxima and minima share some similarity, but the trends differ markedly. The LH curves
 208 (red lines) exhibit both a steady increase, whereas the LA-HadISST curves (black lines) tend
 209 to decline in the first 10–20 years, and to vary at a mostly constant level (Fig.2a and 2b). In
 210 this case, the “story told” by LH is considerably different than that of LA-HadISST.

211 The time series of the SST averaged across the stations from Station 15 (Pingtan) to Station
 212 19 (Yunwo) along the East China Sea coast, where LA-HadISST indicated a stronger
 213 warming than in the LH, is shown in Fig. 2c. The local data indicate markedly lower
 214 temperatures, which may mainly be because of coastal upwelling (the effect of upwelling will
 215 be discussed in the Section 5), but also other local effects, including local tidal mixing, ocean
 216 fronts, sea water vertical mixing, and fresh water discharge, etc., but also a weaker trend (0.18
 217 °C per decade) than in the LA-HadISST (0.35 °C per decade).

218 **Table 3.** Statistics of the time series of the localized SST-analysis (LA-HadISST) data series at the 26
 219 station, as well as the differences (Diff) between statistics of the LH series given in Table 1. The correlation
 220 coefficients between LH and LA-HadISST are also calculated (the 90% confidence level is 0.22, without
 221 considering serial correlation). Red numbers indicate that the correlation coefficients do not conflict with
 222 the null hypothesis of no correlation.

Station No.	Mean LA-HadISST	Diff	Std deviation LA-HadISST	Diff	Trend (°C/10yrs)	Diff	Corr
1	12.80	-1.32	0.43	-0.06	-0.02	0.25	0.20

2	12.93	-0.72	0.37	0.21	0.02	0.24	0.31
3	13.45	-1.76	0.46	0.38	0.13	0.16	0.73
4	13.86	-2.30	0.51	0.07	0.15	0.07	0.67
5	13.71	-0.24	0.54	0.28	0.11	0.11	0.66
6	13.92	-1.12	0.57	0.01	0.14	0.03	0.69
7	14.87	-2.58	0.58	0.01	0.19	-0.05	0.70
8	14.51	0.01	0.54	0.10	0.14	0.03	0.77
9	14.51	-0.60	0.54	0.08	0.14	0.08	0.66
10	16.05	-1.07	0.47	0.10	0.21	0.00	0.71
11	19.70	-2.00	0.57	0.08	0.12	0.14	0.63
12	20.66	-2.65	0.59	0.05	0.27	-0.03	0.67
13	20.66	-2.12	0.59	-0.03	0.27	-0.10	0.64
14	22.47	-2.30	0.70	0.01	0.35	-0.14	0.73
15	23.43	-3.00	0.75	-0.14	0.34	-0.15	0.65
16	23.43	-1.45	0.77	-0.25	0.40	-0.23	0.75
17	22.03	-2.41	0.77	-0.26	0.40	-0.21	0.78
18	24.46	-3.26	0.59	-0.14	0.30	-0.17	0.59
19	24.46	-3.08	0.59	-0.15	0.30	-0.17	0.66
20	25.44	-2.82	0.46	-0.02	0.20	-0.05	0.83
21	25.66	-1.78	0.51	-0.01	0.07	0.11	0.56
22	25.11	-1.47	0.31	0.24	0.07	0.11	0.53
23	25.11	0.71	0.31	0.13	0.07	0.10	0.41
24	25.65	-1.02	0.40	0.09	0.19	-0.03	0.55
25	25.65	-0.47	0.40	0.09	0.19	-0.03	0.57
26	25.93	0.09	0.43	0.00	0.22	-0.04	0.64



224

225

226 **Figure 2.** The annual mean SST series of LA-HadISST (black line) and LH (red line) from Station 1
 227 (Zhimaowan) (a) and Station 2 (Qinhuangdao) (b); The average annual mean SST series of LA-HadISST
 228 (black line) and LH (red line) from Station 15 (Pingtan) to Station 19 (Yunwo) (c).

229

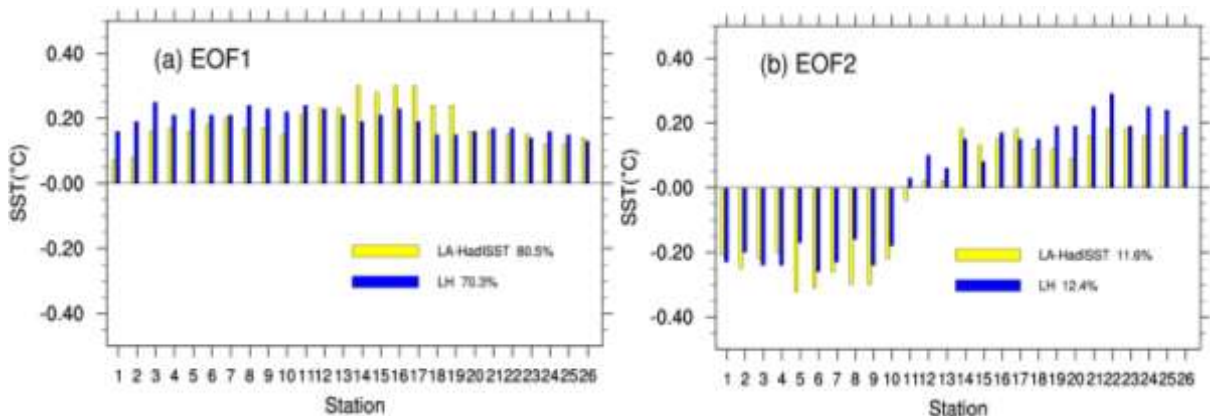
230 The first two EOFs of the LH and the LA data set have similar patterns, namely a uniform
 231 sign along the entire coast in EOF1, with similar intensities, and a north-south dipole (Bohai
 232 Sea and Yellow Sea vs. East and south China Sea) in EOF2, with a sign change at Station 11
 233 (Shipu) (Fig.3a and 3b). The two patterns of LH explain less variance, namely 82.9% of the
 234 total variance, than the LA-HadISST EOFs, which go with 92.9%. This may be related to the
 235 larger spatial variability in local data compared to gridded data. In EOF1, again the Station 1
 236 (Zhimaowan) and Station 2 (Qinhuangdao) in the Bohai Sea contribute less in LA-HadISST,
 237 whereas the Station 15 (Pingtan) to Station 19 (Yunwo) contribute more to the overall
 238 warming than in LA-HadISST than in LH.

239 The time coefficients (PCs) are broadly similar, even if the correlations are not very strong:
 240 only 0.84 and 0.42 (Fig.3c and 3d). A general warming is associated with EOF1 and mostly
 241 stationary inter-annual variability with EOF2. Again, the sequence of maxima and minima is

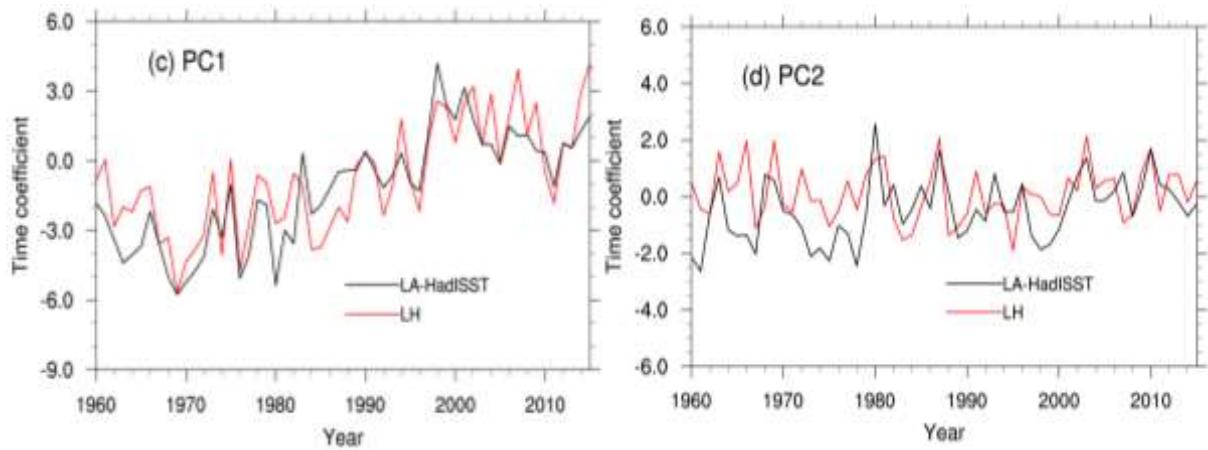
242 qualitatively similar, but PC2 of LA-HadISST exhibits a break point at about 1980 –
 243 interestingly the time when satellites became routinely available of the global analyses. These
 244 data improve SST sampling, especially in the Southern Ocean and coastal areas (Smith et al.,
 245 2008; Lima and Wetthey 2012). Before 1980, PC2 of LH and LA-HadISST differed by about
 246 0.2 (Fig. 3d; this corresponds to a mean difference of 0.04K at the southern stations from
 247 Station 11 to Station 26 during that time, and a mean difference 0.04K at the northern stations
 248 from Station 1 to Station 10 (Fig. 3b)).

249 To further study the differences in trends, EOFs were calculated from the difference time
 250 series, that is, LH anomalies minus LA-HadISST anomalies at the 26 sites (Fig. 4). The first
 251 two EOFs stand for 31.2% and 27.6% of the variance. These numbers are not very different,
 252 and it their closeness may be indicative that the EOFs are degenerate (von Storch and Zwiers
 253 1999). These EOFs describe covariations of the differences along long stretches of the coast;
 254 in case of EOF1, this is the case for all stations at the southern Station 11 (Shipu), i.e., in the
 255 East and South China Sea (Fig.4a). In EOF2 it is all stations at the southern Station 13
 256 (Kanmen), mostly in the Yellow Sea and Bohai Sea (Fig. 4b). PC1 seems to describe a change
 257 point at about 1980, whereas PC2 describes a slight upward trend: The differences tend to be
 258 larger in earlier years and are almost nil in the end of the considered time interval. That is, in
 259 recent years, there are little differences between LA-HadISST and LH, which is not surprising
 260 giving the better observational and reporting practice.

261 That in early years inhomogeneities impacted the quality of SST analyses is also not
 262 surprising, but it is valuable to learn when these inhomogeneities took place, and which time
 263 periods in the analyses should be taken with some reservation. Of course, this assertion
 264 depends on the assumption that the homogenization of the local data did remove all change
 265 points and other inhomogeneities.



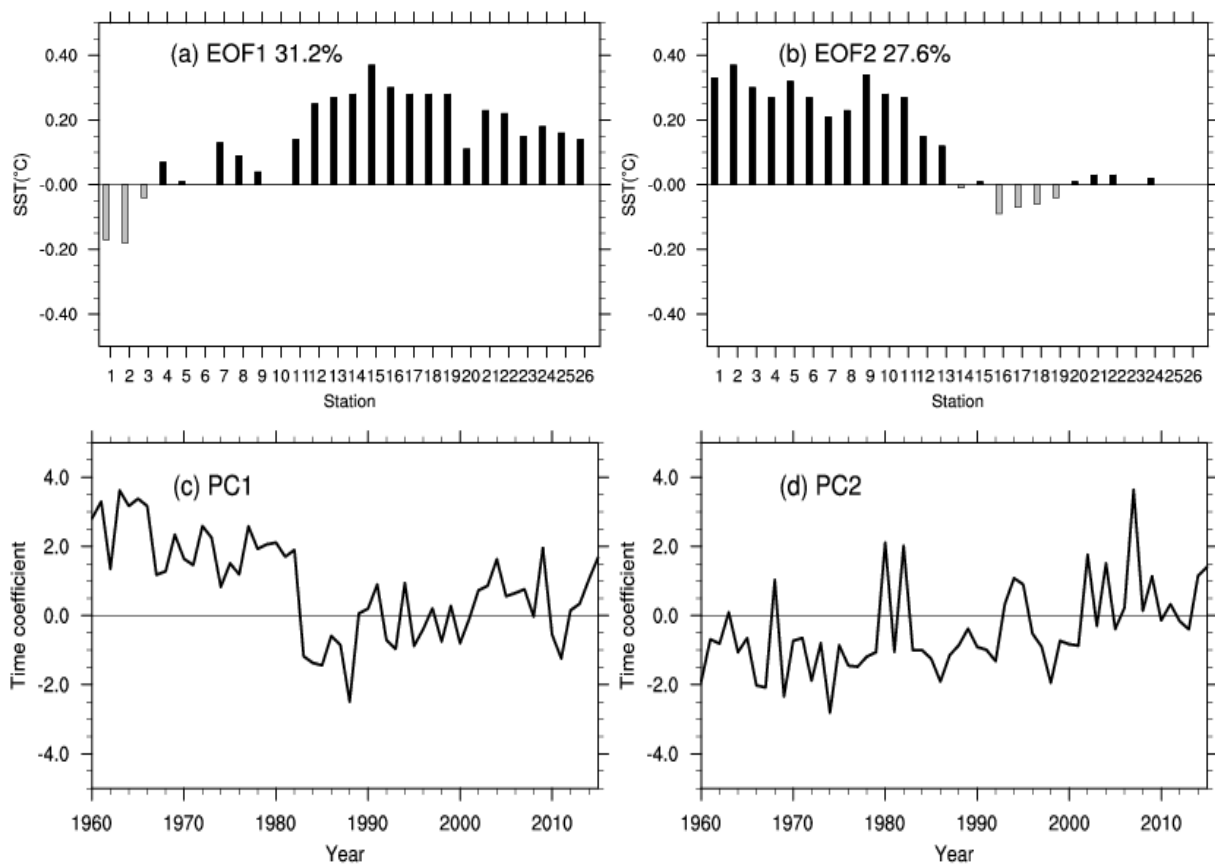
266



267

268 **Figure 3.** Comparison of the EOF1 and EOF2 derived from the LH data set of local SST at 26 sites (blue
 269 bars; red lines), and derived from the localized analysis data LA-HadISST (yellow bars; black lines).
 270 Top: EOF spatial patterns, bottom: principal components (time coefficients).

271



272

273 **Figure 4.** First two EOFs of the difference time series LH-LA-HadISST. Top: EOF spatial patterns, bottom:
 274 principal components (time coefficients).

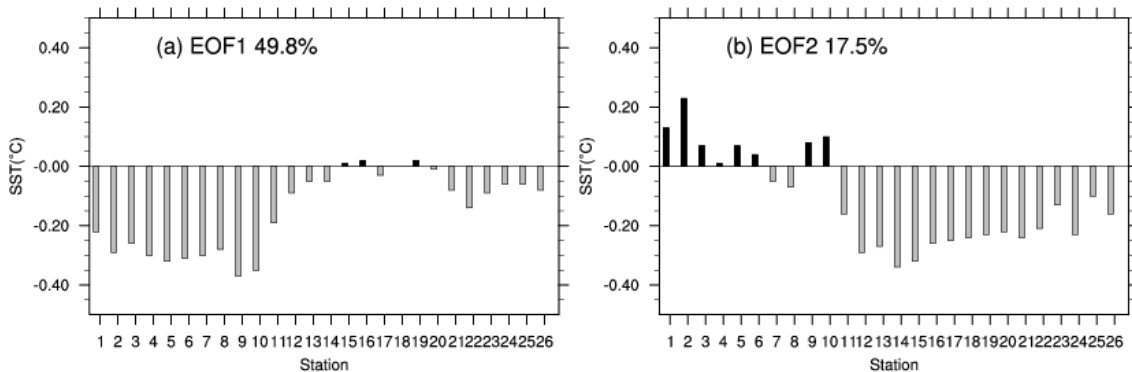
275

276 **4.2 Comparing with COBE SST**

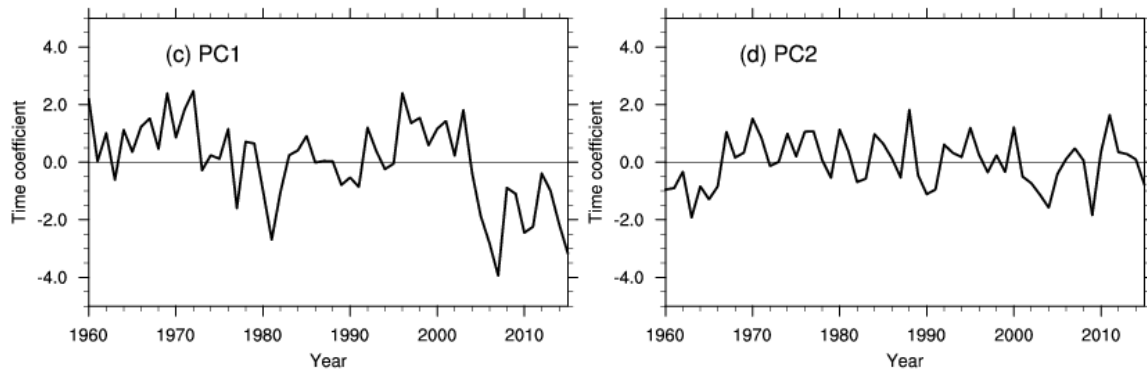
277 In this subsection, we consider the localized SST derived from the LA-COBE SST data set
278 during 1960–2015. Again, the LA-COBE SST is in almost all sites higher than the local data,
279 namely at 21 out of 26 sites. The differences are up to 3K, and again mostly along the East
280 China Sea coast from Station 11 (Shipu) to Station 20 (Zhelang) (see Table SOM-1 in the
281 Supplementary Online Material (SOM)). The local correlations are relatively high, namely
282 between 0.55 and 0.85.

283 The EOFs derived from the LA-COBE SST, with the same grid resolution of 1° and the same
284 time window 1960–2015 as LA-HadISST, exhibits broadly the same pattern in space and time
285 as the EOFs of the LH data. Also, the explained variances are close (Figure SOM-2). The
286 northern stations contribute more to the overall warming represented by EOF1, whereas the
287 stations along the South and East China Sea contribute less. Again, the two northernmost
288 Station 1 (Zhimaowan) and Station 2 (Qinhuangdao) exhibit some systematic differences,
289 both in EOF1 and EOF2. The PCs share correlations of 0.80 for EOF1 and 0.50 for EOF2.
290 COBE SST does not capture the recovery of the dip in warming since about 2000, as LH and
291 HadISST did, while EOF2 reveals some warming in the final years. During the 1960s some
292 differences prevail.

293 Fig.5 shows the EOFs of the difference time series between LH anomalies and LA-COBE
294 SST anomalies. The first EOF dominates, with 49.8%, whereas the second one represents a
295 share of 17.5%. The first EOF points to several inhomogeneities, with two prolonged intervals
296 during which LH is higher than LA-COBE SST (i.e., 1960–1978, and 1995–2005), and a
297 strong drop-down to negative PC-values after about the year of 2005. PC2, on the other hand,
298 appears as mostly stationary, except for a suspiciously negative episode in the early 1960s.



299



300

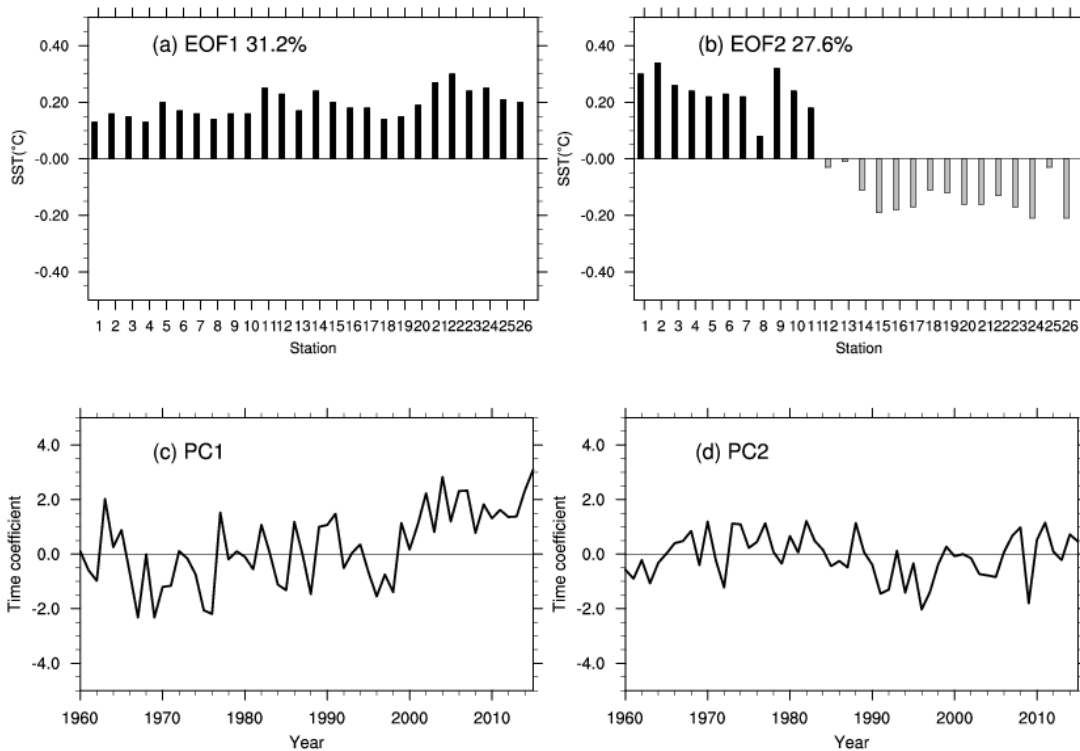
301 **Figure 5.** EOF analysis of the differences LH-LA-COBE: Top: EOF spatial patterns (EOFs), bottom:
 302 principal components (time coefficients).

303 4.3 Comparing with ERSST

304 ERSST presents SST on a coarser grid compared to the two cases before. Again, the
 305 temperatures given by ERSST, as was the case with the other two analyses, are higher than
 306 the temperatures recorded at the local sites along the coast (see Table SOM-2). The
 307 differences are up to 4K, and the largest differences are found in the East China Sea from
 308 Station 11 (Shipu) to Station 20 (Zhelang). That the differences are in this case even larger
 309 than in the other LA cases may be related to the 2° coarse resolution of ERSST.

310 The variability according to ERSST is quite similar to that of LH, at least in terms of EOFs
 311 (see Figure SOM-3). The correlation of the PC1's is 0.83, and of PC2's to 0.60. LA-HadISST
 312 got 0.84 and 0.42, LA-COBE SST got 0.80 and 0.50. The local correlations vary between 0.37
 313 and 0.82. Again EOF1 stands for an overall warming and EOF2 to interannual variability with
 314 hardly a trend. The relative contributions of the two EOFs compare well to the LH-EOFs. In
 315 detail, the northernmost stations appear stronger in EOF1 of LA-ERSST than in that of LH,
 316 whereas the northern sites are underrepresented, and the southern over-represented in EOF2.

317 The EOFs of the differences between LH anomalies and LA-ERSST anomalies are shown in
 318 Fig. 6. They differ strongly from those found for LA-COBE SST and LA-HadISST. The first
 319 EOF differences resemble the first EOFs of LH and LA-ERSST (not shown; see Fig. SOM-3)
 320 – the long-term trend in LA-ERSST is smaller than in the local data – everywhere. The
 321 second EOF is again a dipole pattern, with the Bohai Sea and the Yellow Sea on the one side,
 322 and the East China Sea and South China Sea on the other. The time series of PC2 fluctuates
 323 around zero without prominent long-term trend.



324

325

326 **Figure 6.** EOF analysis of the differences LH-LA-ERSST: Top: EOF spatial patterns (EOFs), bottom:
 327 principal components (time coefficients).

328

329 **5 Discussion and conclusion**

330 We have mainly examined three global gridded analysis SST data sets in the Chinese coastal
 331 waters. For doing so, we have compared a number of statistical properties for 26 coastal
 332 hydrological locations as given by the analyses and by a newly digitized and homogenized
 333 data set (Li et al., 2018). For demonstrating the utility of the local data set, we have compared
 334 the local SST series (named LH) with independent local homogenized SAT data from nearby
 335 meteorological stations. The variations of the two series are fully consistent. Another
 336 argument points to the quality of the LA data set is that the differences between LH and the
 337 three LAs (localized data from the different global analyses: HadISST1, COBE SST, ERSST)
 338 considered are not uniform (except for the time mean); instead the LAs deviate in different
 339 ways from LH. If this would not be the case, one could be tempted to argue that the
 340 differences are manifestations of inefficiencies of the LH data set. This is not the case.

341 In this study, we found that all of these globally gridded datasets exhibit surface temperatures
 342 usually higher than the LH data, especially at the East China Sea. This difference may be
 343 caused by two factors. In the China Seas, most of the coastal upwelling currents occur at the
 344 East China Sea and the northern South China Sea, other small upwelling currents at the tops

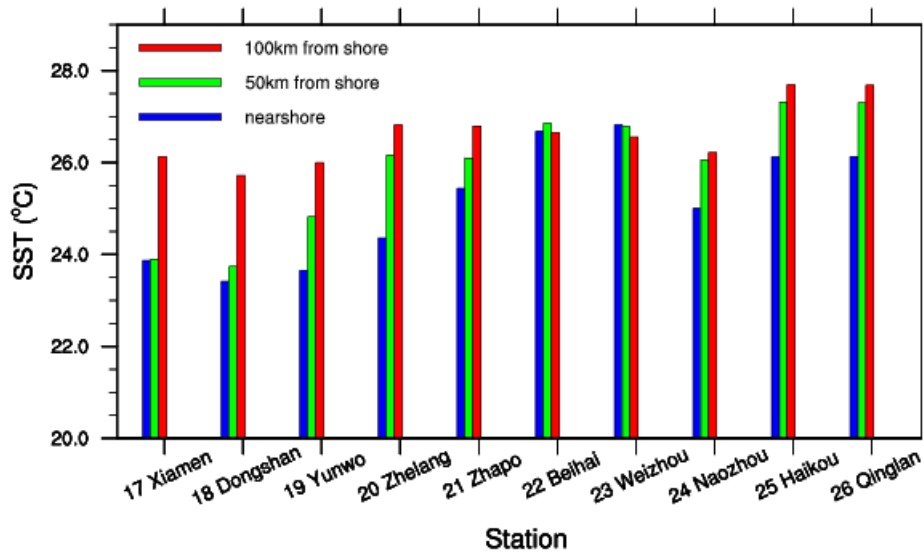
345 of the Liaodong Peninsula and Shandong Peninsula (Figure 1) (Yan 1991). The consensus of
346 previous studies is that coastal upwelling currents results in cooling SST at these coastal areas
347 (Xie et al, 2003; Guan et al., 2009; Su et al., 2012). In our study, we find that the in-situ
348 shoreline SSTs at the upwelling areas (e.g. Station 4 (Laohutan), Station 11 (Shidao) and
349 Station 18 (Dongshan)) are always colder than global gridded SST data, with the value of
350 below -1K (Table 2, Table 3 and Table SOM1).

351 We hypothesize that these negative differences are connect by coastal upwelling currents. To
352 test this hypothesis, we examine the output of a numerical simulation of the currents in the
353 South China Sea with a grid resolution of 0.04° . The model is embedded in an almost global
354 model with 1° grid resolution (Tang et al., 2018). The model used here is the Hybrid
355 Coordinate Ocean Model (HYCOM) that is exposed to periodic climatological atmospheric
356 forcing, with a fixed annual cycle but no weather disturbances. The atmospheric forcing
357 comes from the International Comprehensive Ocean-Atmosphere Data set (ICOADS). We
358 extract simulated SSTs at three different distances (i.e., near the station, 50 km, and 100 km
359 from each coastal hydrological station in South China Sea). Fig.7 shows that most shoreline
360 SSTs are lower than ambient offshore SSTs, especially SSTs at 100km from shoreline.
361 However, the Stations 22 (Beihai) and Station 23 (Weizhou) are not affected by coastal
362 upwelling, and consistently, there are no notable differences among SSTs at three different
363 distances from the two stations. The result reflects that the homogenized SST data set for
364 shoreline stations catches this relative cooling water effect of the regional upwelling currents.
365 On the other hand, the global gridded SST datasets point to higher temperatures which may be
366 caused by their coarse resolution. The differences are largest in the case of the coarsest
367 analysis (ERSST), but weakest in the OISST v2 analysis with a resolution of 0.25° (Fig. 8; see
368 below) (Note that the difference of LH minus LA-OISST is restricted to the warmer episode
369 1982–2015). Meanwhile, the lack of near-shore observations when compiling near-shore box
370 averages in coastal areas may also cause these differences (Wang et al., 2018). Besides, there
371 still some other local mechanisms with smaller scale can cause cooling water in the China
372 Seas, such as China coastal current (CCC) (Belkin and Lee, 2014) and ocean fronts (Zhao,
373 1987; Hickox et al., 2000). In them, the shallow water shelf front and estuarine plume front
374 are two major fronts in the Bohai Sea and the Yellow Sea in summer. Coastal current front,
375 upwelling front as well as strong westerly boundary current usually appears in the East China
376 Sea and the South China Sea which may also be related to coastal upwelling currents.

377 In summary, our main results are as follows:

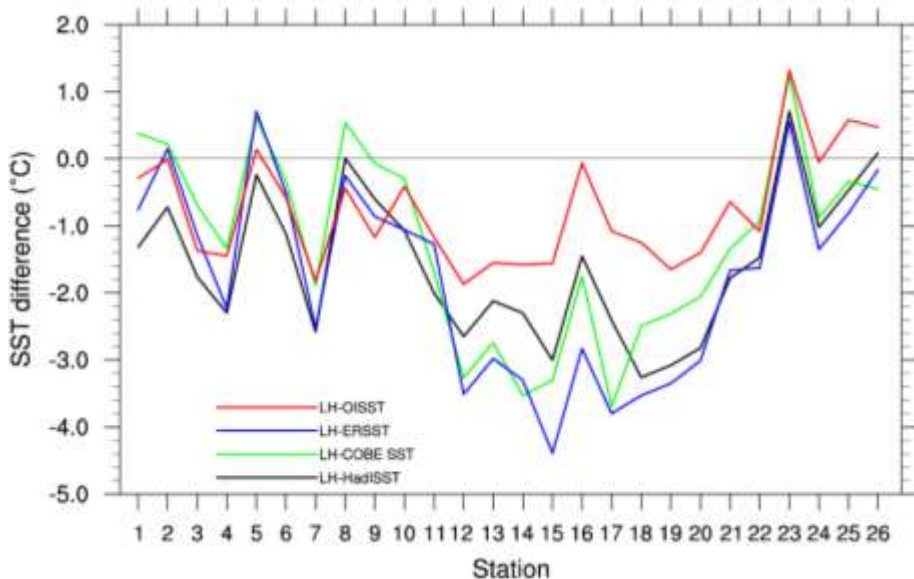
- 378 – The mean SST in LH at many sites is considerably lower than that in the LA-data sets.
379 We suggest that this is related to local oceanic effects, such as coastal upwelling. The
380 LA-datasets cannot catch this cooling effect of the regional upwelling currents well.
381 On the other hand, the global gridded SST datasets point to higher temperatures which
382 may be caused by their coarse resolution when averaging in the LA data sets. However,
383 systematic differences would not be expected to influence strongly the overall
384 variability and trends.
- 385 – The first EOF in all data sets stands for a general warming, and the second for
386 interannual variability. This is not only so in the local LH-data but also in all globally
387 gridded-based LA-datasets.
- 388 – In the years following the introduction of satellites in monitoring SST, since about
389 1980, the different global analyses converge, and the differences to the local data set
390 become smaller. In support of this, the comparison with the high resolution analysis
391 OISST v2 for the post-satellite period 1982–2015 reveals few differences (not shown,
392 see Fig. SOM-4).
- 393 – In the years before 1980, some noteworthy differences are found. The differences
394 between the LH-data anomalies and the LA-data anomalies are non-uniform across the
395 different LA data sets. For instance, for ERSST the long-term trends differ, in case of
396 COBE SST several jumps emerge, and in case of HadISST, a jump is found at the time
397 of the advent of the routine satellite data, but also a trend in PC2 of the differences.

398 Thus, our overall conclusion is that the global gridded SST datasets correctly describe the
399 main features of variabilities and trends in regional waters, but that significant improvements
400 in the regional analyses may be gained when quality controlled homogenized data are
401 incorporated. In particular for the time prior to the usage of remote sensing by satellites, and
402 in regions where observational efforts have been limited, such efforts are valuable
403 contributions to climate variability and change studies. Our example should also be an
404 encouragement for national climate services to revisit regional data, and to invest into the
405 elimination of inconsistencies caused by inhomogeneities. There are several projects or
406 researches dedicated quality control and homogenization of *in situ* data (Kuglitsch et al., 2012;
407 Hausfather et al., 2016; Minola et al., 2016). It is useful to keep some high-quality data
408 separate from that available for analyses, for validation activities such as our work and others'
409 work (Hausfather et al., 2017).



410

411 **Figure 7.** Simulated SSTs at different distances from each coastal hydrological station in the South China
 412 Sea.



413

414 **Figure 8.** The mean SST differences at the 26 locations between LH and LA-OISST (1982-2015; red
 415 line), LH and LA-ERSST (1960-2015; blue line), LH and LA-COBE SST (1960-2015; green line) and
 416 LH and LA-HadISST (1960-2015; black line)

417

418 *Data availability.* All the four gridded SST analyses used in this study are publicly available
 419 and can be downloaded freely from the websites shown in Table 1. The observational in situ
 420 SST data from the coastal stations and the coordinates of coastal stations can be obtained from
 421 the National Marine Science Data Center, National Science & Technology Resource Sharing
 422 Service Platform of China (<http://mds.nmdis.org.cn>). However, the observational in situ SST

423 data from only 9 coastal stations are publicly available. SST data from the rest stations can be
424 obtained after an application to the website.

425 *Acknowledgments.* The work is funded by the program of National Natural Science
426 Foundation of China (No. 41376014; No. 41706020), the National Key Research and
427 Development Program of China (No.2018YFA0605603; No. 2017YFC1404700) and also
428 supported by the Hamburg University's Cluster of Excellence CliSAP in Germany,
429 Shengquan Tang's work is funded by the Chinese Scholarship Council.

430

431 **References**

432 Belkin, I. M.: Rapid warming of Large Marine Ecosystems, *Progr Oceanogr*, 81(2009),
433 207-213, 2009.

434 Belkin, I.M., Lee, M.-A. Long-term variability of sea surface temperature in Taiwan Strait.
435 *Climatic Change*, 124 (4), 821-834, 2014.

436 Burrow, M. T., et al. The pace of shifting climate in marine and terrestrial ecosystems,
437 *Science*, 334, 652-655, 2011.

438 Bungel, L. and Clarke, Allan J.: A verified estimation of the El Niño index Niño-3.4 since
439 1877, *J. Climate*, 22(14), 3979-3992, 2009.

440 Guan, J., Cheung, A., Guo, X. and Li, L. Intensified upwelling over a widened shelf in the
441 northeastern South China Sea, *J. Geophys. Res.*, 114, 2009.

442 Harris, I., Jones, P. D., Osborn, T.J., and Lister, D.H.: Updated high-resolution grids of
443 monthly climatic observations- the CRU TS3.10 dataset, *Int. J. Climatol.* 34, 623-642,
444 2014.

445 Hausfather, Z. and Coauthors: Assessing recent warming using instrumentally
446 homogeneous sea surface temperature records. *Sci. Adv.*, 3, 31601207, 2017.

447 Hausfather, Z., Cowtan, K. Menne, M. J. and Williams Jr., C. N.: Evaluating the impact of
448 U.S. Historical Climatology Network homogenization using the U.S. Climate Reference
449 Network, *Geophys. Res. Lett.*, 43, 1695–1701, 2016.

450 Hickox, R., Belkin, I.M., Cornillon, P., Shan, Z. Climatology and seasonal variability of
451 ocean fronts in the East China, Yellow and Bohai seas from satellite SST data. *Geophys.*
452 *Res. Letters*, 27(18), 2945-2948, 2000.

453 Hiraharas, S., Ishii, M., and Fukuda, Y.: Centennial-Scale Sea Surface Temperature
454 Analysis and Its Uncertainty, *J. Climate*, 27, 57-75, 2014.

455 Honkoop R.J.C., der Meer, J.Van, Beukema, J. J. and Kwast D. Does temperature-
456 influenced egg production predict the recruitment in the bivalve *Macoma Balthica*? *Mar.*
457 *Ecol. Prog. Ser.*, 64, 229-235,1998.

458 Huang B., and Coauthors. Extended Reconstructed Sea Surface Temperature version 4
459 (ERSST v4). Part I: Upgrades and intercomparisons. *J. Climate*, 28,911-930, 2015.

460 Ishii, M., Shouji, A., Sugimoto, S., and Matsumoto, T.: Objective analyses of sea-surface
461 temperature and marine meteorological variables for the 20th century using ICOADS
462 and the Kobe Collection, *Int. J. Climatol.*, 25, 865-879, 2005.

463 Jin, Q. H. and Wang, H.: Multi-time scale variations of sea surface temperature in the China
464 Seas based on the HadISST dataset, *Acta. Oceanol. Sin.*, 30, 14-23, 2011.

465 Kim, K.Y., North, G.R. and Huang, J.P.: EOFs of one dimensional cyclostationary time
466 series: Computation, examples, and stochastic modeling, *J. Atmos. Sci.*, 53, 1007-1017,
467 1996.

468 Kuglitsch, F.G., Auchmann, R., Bleisch, R., Bronnimann, S., Martius, O., and Stewart, M.:
469 Break detection of annual Swiss temperature series. *J. Geophys. Res.*, 117(D13105), 1-
470 12, 2012.

471 Li, Y., Wang, G.S., Fan, W.J., Liu, K.X., Wang, H., Tinz, B., von Storch, H., and Feng, J. L.:
472 The homogeneity study of the sea surface temperature data along the coast of the China
473 Seas, *Acta. Oceanol. Sin.* 40, 17-28, 2018 (in Chinese but with English abstract).

474 Li, Y., Mu, Lin, Liu, Y. L., Wang, G.S., Zhang, D.S., Li, H., Han, X. Analysis of variability
475 and long-term trends of sea surface temperature over the China Seas derived from a
476 newly merged regional data set. *Climate Research*, 73, 217-231, 2017.

477 Lima, F.P. and Wethey, D.S. Three decades of high-resolution coastal sea surface
478 temperatures reveal more than warming, *Nat. Commun.*, 3,704, 2012.

479 Liu, Q.Y. and Zhang, Q.: Analysis on long-term change of sea surface temperature in the
480 China Seas, *J. Ocean University China* 12, 295-300, 2013.

481 Mantua, N.J. and Hare, S.R.: The Pacific decadal oscillation, *J. Oceanogr.*, 58, 35-44, 2002.

482 Minola, L., Azorin-Molina, C., and Chen, D. L.: Homogenization and assessment of
483 observed near-surface wind speed trends across Sweden, 1956-2013. *J. Clim.*, 29(20),
484 7397-7415, 2016.

485 Rayner, N.A., Parker, D.E., Horton, E.B., and others: Global analyses of sea surface
486 temperature, sea ice, and night marine air temperature since the late nineteenth century,
487 *J. Geophys. Res.*, 108(D14),1063-1082, 2003.

488 Reynolds, R.W., Smith, T.M., Liu, C.Y., Chelton, D.B., Casey, K.S. and Schlax, M.: Daily
489 high-resolution-blended analyses for sea surface temperature, *J. Climate*, 20, 5473-5496,
490 2007.

491 Park, K. A., Lee, E.Y., Chang, E., and Hong, S.: Spatial and temporal variability of sea
492 surface temperature and warming trends in the Yellow Sea. *J. Mar. Sys.* 143, 24-38,
493 2015.

494 Saji, N. H., Goswami, B. N., Vinayachandran, P.N., Yamagata, T.: A dipole mode in the
495 tropical Indian Ocean, *Nature* 401, 360-363, 1999.

496 Sen, P.K.: Estimates of regression coefficient based on Kendall's tau, *J. Am. Stat. Assoc.* 63,
497 1379-1389, 1968

498 Smith, T.M., Reynolds, R.W., Peterson, T.C. and Lawrimore, J.: Improvements to NOAA's
499 historical merged land-ocean surface temperature analysis (1880-2006), *J. Climate*,
500 21(10), 2283-2296, 2008.

501 Su, J., Xu, M., Pohlmann, T., Xu D., Wang D. A western boundary upwelling system
502 response to recent climate variation (1960–2006), *Cont. Shelf Res.*, 57(2013)3-9, 2012.

503 Tang, S., von Storch, H. Chen, X., and Zhang, M. "Noise" in climatologically driven ocean
504 models with different grid resolution, *Oceanologia*, 10.1016/j.oceano.2019.01.001,
505 2019.

506 Tokinaga, H., Xie, S.P., Deser, C., Kosaka, Y. and Okumura, Y. M.: Slowdown of the
507 Walker circulation driven by tropical Indo-Pacific warming, *Nature*, 491(7424), 439-43,
508 2012.

509 Vecchiga, Clement, A., Soden, B.J.: Examining the Tropical Pacific's Response to Global
510 Warming, *Eos Transactions American Geophys Union*, 89(9), 81–83, 2008.

511 Von Storch, H. and Zwiers, F.W.: *Statistical analysis in climate research*. Cambridge
512 University Press: London, 1999.

513 Wang, Q.Y., Li, Y., Li, Q.Q., et al. A comparison and evaluation of two centennial-scale sea
514 surface temperature datasets in the China Seas and their adjacent sea areas, *J. Trop.*
515 *Meteor.*, 24(4), 452-460, 2018.

516 Wernberg, T., Bennett, S., Babcock, R.C., et al. Climate-driven regime shift of a
517 temperature marine ecosystem, *Science*, 353, 169–172, 2016.

518 Wu, L. X., Cai, W. J., Zhang, L.P., and others: Enhanced warming over the global
519 subtropical west boundary currents, *Nat. Clim. Change*, 2(3), 161-166, 2012.

520 Xie, S.P., Xie, Q., Wang, D., and Liu, W.T. Summer upwelling in the South China Sea and
521 its role in regional climate variations, *J. Geophys. Res.*, 108(C8), 3261,
522 doi:10.1029/2003JC001867, 2003.

523 Xie, S.P., Clara, D., Gabriel, A. V., Ma, J., Teng, H.Y. and Andrew, T. W.: Global warming
524 pattern formation: sea surface temperature and rainfall, *J. Climate*, 23(4), 966-986,
525 2010.

526 Xu, W.H., Li, Q.X., Wang, X.L., Yang, S., Cao, L.J. and Feng, Y.: Homogenization of
527 Chinese daily surface air temperature and analysis of trends in the extreme temperature
528 indices, *J. Geophys. Res.*, 118(17), 9708-9720, 2013.

529 Yan, T.Z. A preliminary classification of coastal upwellings in the China Seas. *Mar. Sci.*
530 *Bull.*, 10(6), 1-6, 1991. (in Chinese with English abstract)

531 Yeh, S.W. and Kim, C. H.: Recent warming in the Yellow/East China Sea during winter and
532 the associated atmospheric circulation, *Cont. Shelf Res.*, 30, 1428-1434, 2010.

533 Zhao, B.R., Ren, G.F., Cao, D.M., Yang, Y.L. Characteristics of the ecological environment
534 in upwelling area adjacent to the Changjing River Estuary, *Oceanol. Limnol. Sin.*, 32(3),
535 327-333, 2001. (in Chinese with English abstract)

536

537 **Appendix A: Consistency of homogenized SST data set with homogenized SAT data set**

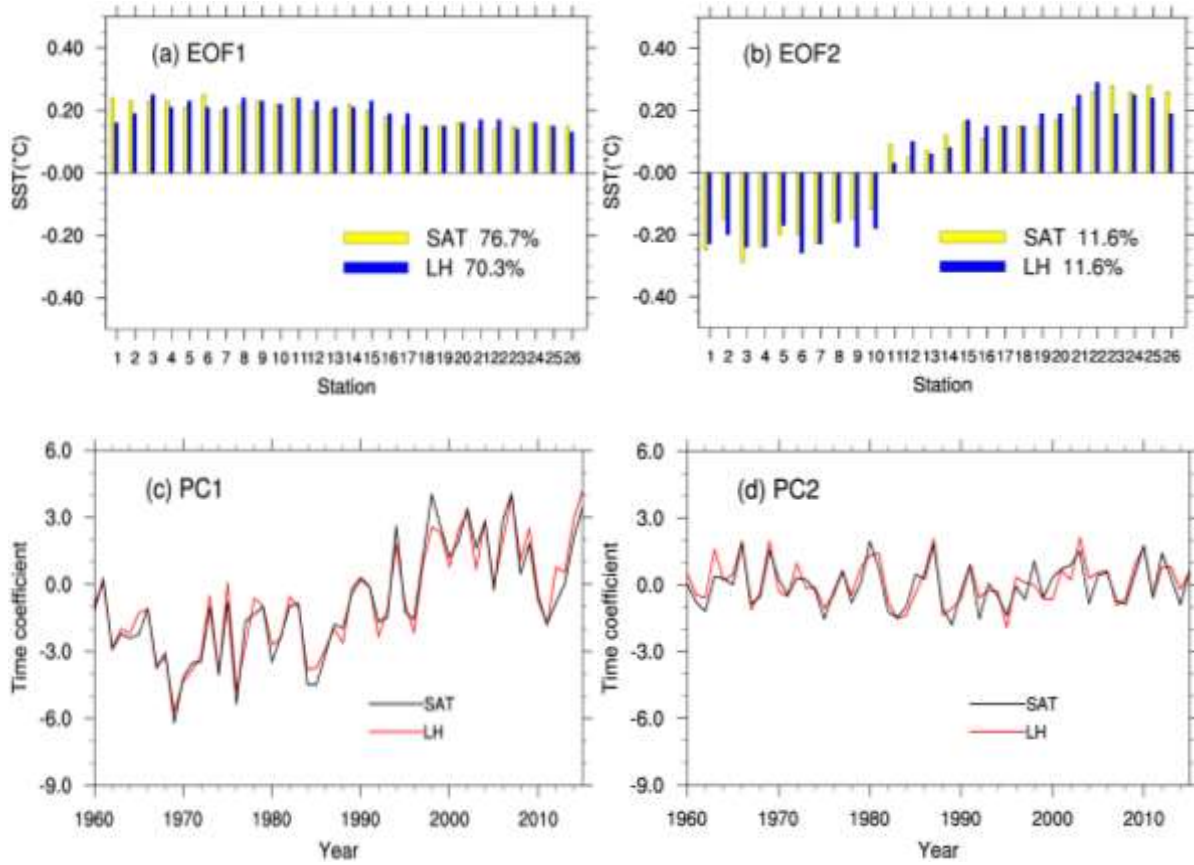
538 We examine if the SST data is consistent with other local homogenized data, specifically with
539 time series of surface air temperature (SAT) at various locations along the Chinese coast. This
540 data set contains data from many sites. For each of the SST measuring sites, there is at least
541 one SAT stations within 100 km distance. We form 26 pairs of located SST/SAT data. SST
542 and SAT data directly are not compares pairwise, but in terms of the patterns and coefficient
543 time series (PCs) of their empirical orthogonal functions (EOFs).

544 The first EOFs of SST and *in situ* SAT describe an overall warming, with a slight tendency of
545 stronger warming in terms of both SST and SAT in the northerly Bohai and Yellow Sea (Fig.
546 A1a). This pattern is dominant, representing 70.3% and 76.7% of the total interannual
547 variance. The warming is mostly continuous from about 1970 until 2010 (Fig. A1c). The
548 similarity of the principal components – expressed by 0.97 in terms of the correlation
549 coefficient – is striking (Fig. A1c). The second EOFs represent considerably less variance –
550 namely about 11.6% (Fig. A1b). They describe a North-South contrast, and stationary PCs,
551 varying around 0 without prolonged positive or negative excursions (Fig. A1d). Also the PCs
552 of the second PCs of SST and SAT show a remarkably parallel development – with a high
553 correlation of 0.86 (Figs.A1d).

554 When this exercise is repeated with CRU TS 3.24.01 instead of the *in situ* SAT series, we find
555 similar consistency (see Fig. SOM-1). The PCs of SAT-CRU also show high correlations of
556 0.94 and 0.83 with the *in situ* SST (see Fig. SOM-1).

557 We conclude that the two data sets are consistent; the first EOFs describe the warming of the
558 recent decades of years; the second EOFs describe interannual variability, and may be
559 influenced by ENSO and other patterns of natural variability. We furthermore conclude that
560 the new description of SST variability and trends at the 26 sites along the Chinese coast
561 presents a reliable account of the past since 1960 – and thus may serve as a benchmark for
562 assessing global analyses of SST datasets.

563



564

565

566 **Fig. A1.** Comparison of the EOF1 and EOF2 derived from the LH data set of local SST at 26 sites (blue
 567 bars; red lines), and derived from the SAT at the same sites (yellow bars; black lines).
 568 Top: EOF spatial patterns, bottom: principal components (time coefficients).

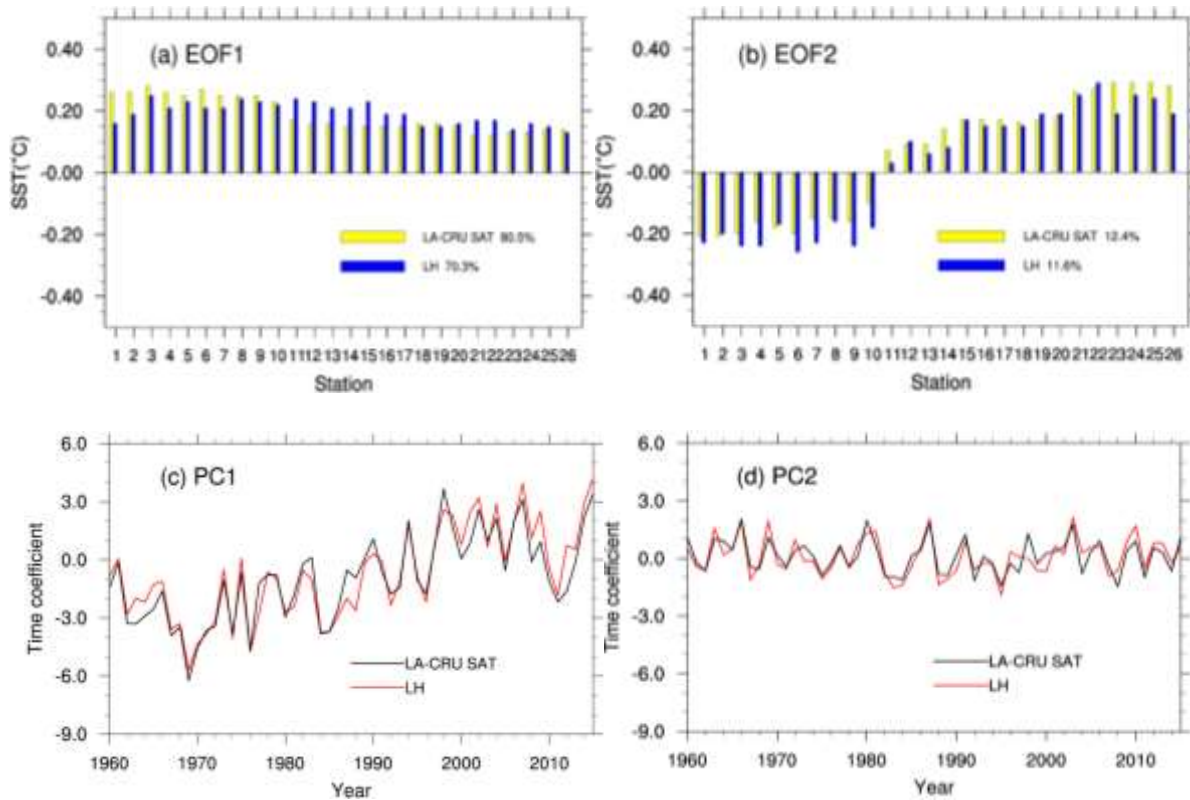
569

570

571

Appendix B: Supplementary Online Material (SOM)

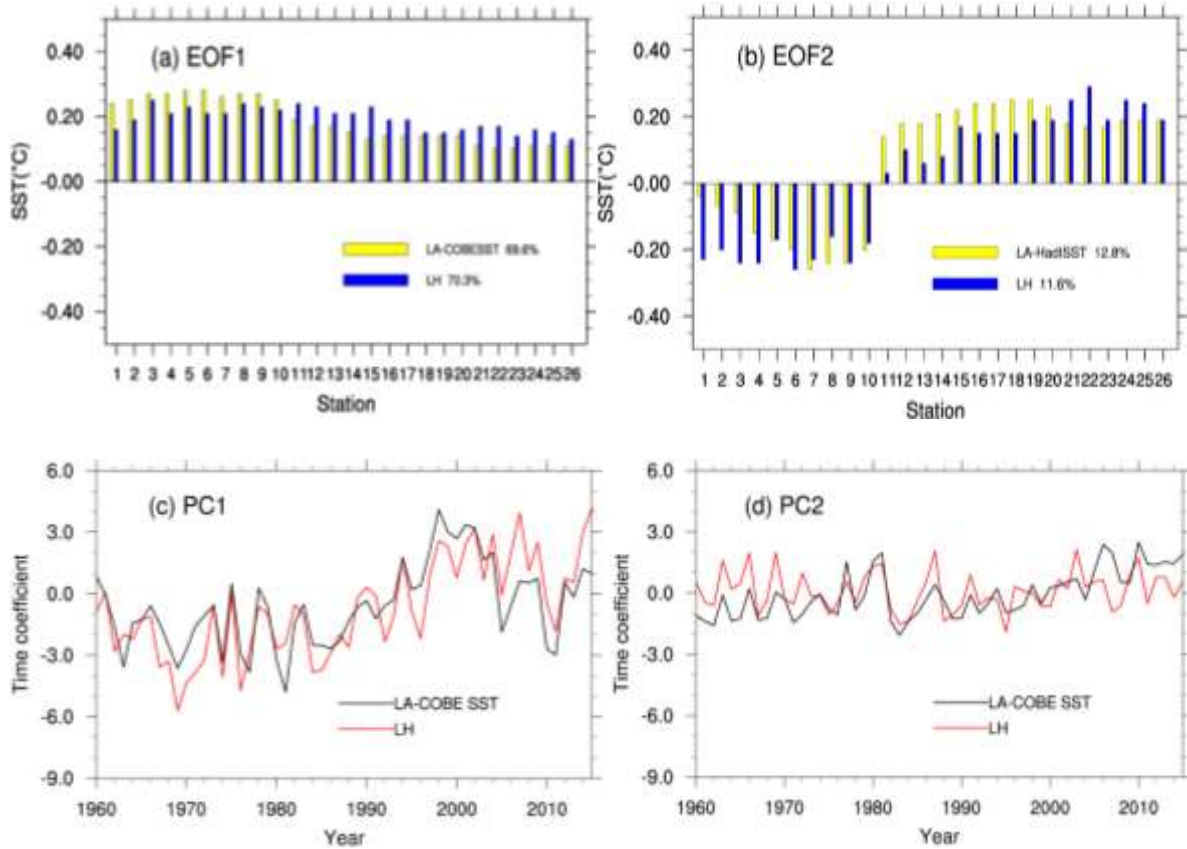
572



573

574

575 **Fig. SOM-1.** Comparison of the EOF1 and EOF2 derived from the LH data set of local SST at 26 sites
576 (blue bars; red lines), and derived from the CRU SAT at the same sites (yellow bars; black lines).
577 Top: EOF spatial patterns, bottom: principal components (time coefficients).
578

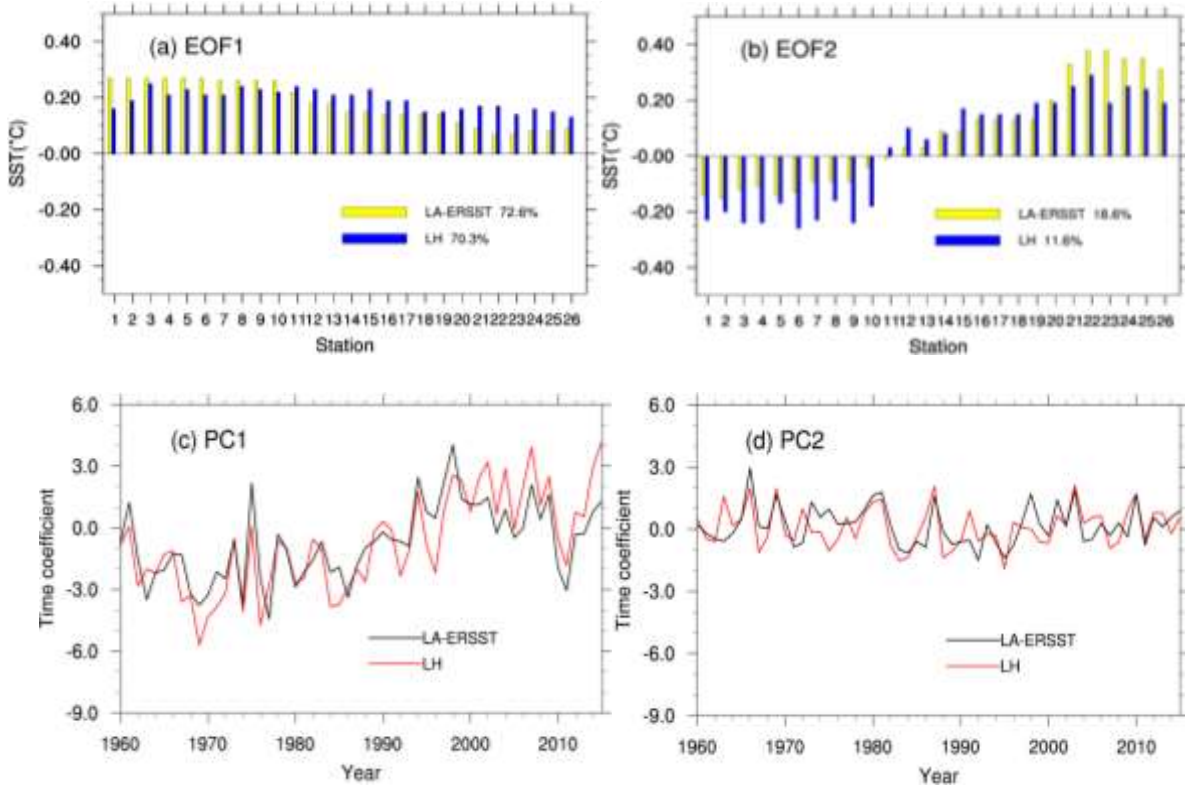


579

580

581 **Fig. SOM-2.** Comparison of the EOF1 and EOF2 derived from the LH data set of local SST at 26 sites
 582 (blue bars; red lines), and derived from the localized analysis data LA-COBE SST (yellow bars; black
 583 lines). Top: EOF spatial patterns, bottom: principal components (time coefficients).

584



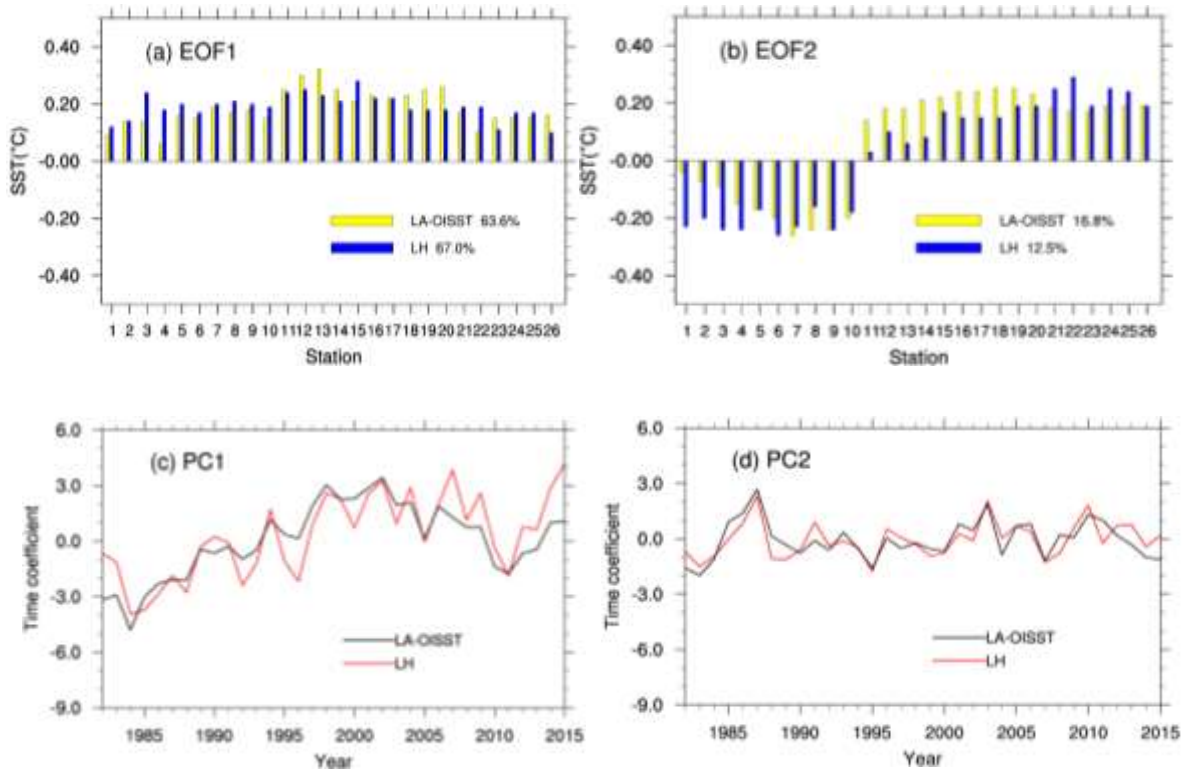
585

586

587

588 **Fig. SOM-3.** Comparison of the EOF1 and EOF2 derived from the LH data set of local SST at 26 sites
 589 (blue bars; red lines), and derived from the localized analysis data LA-ERSST (yellow bars; black lines).
 590 Top: EOF spatial patterns, bottom: principal components (time coefficients).

591



592

593

594 **Fig. SOM-4.** Comparison of the EOF1 and EOF2 derived from the LH data set of local SST at 26 sites
 595 (blue bars; red lines), and derived from the localized analysis data LA-OISST (yellow bars; black lines).
 596 Top: EOF spatial patterns, bottom: principal components (time coefficients).

597

598 Table SOM-1. Statistics of the time series of the localized SST-analysis (LA-COBE SST) data series at the
599 26 station, as well as the differences (Diff) between the pairs of time series. The correlation coefficients
600 between LH and LA-COBE SST are also calculated (the 90% confidence level is 0.22, without considering
601 serial correlation). Red numbers indicate that the correlation coefficients do not exceed the 90% confidence
602 level.

No	Mean LA-COBE SST	Diff	Std-dev LA-COBE SST	Diff	Trend (°C/10yrs)	Diff	Corr
1	11.13	0.38	0.52	0.01	0.17	0.00	0.60
2	11.99	0.22	0.54	0.04	0.16	0.10	0.56
3	12.23	-0.69	0.56	0.14	0.14	0.15	0.74
4	12.70	-1.34	0.59	0.00	0.10	0.11	0.59
5	12.75	0.61	0.60	-0.01	0.10	0.12	0.64
6	12.98	-0.33	0.61	-0.03	0.07	0.10	0.66
7	13.98	-1.89	0.61	-0.02	0.01	0.13	0.68
8	13.83	0.54	0.62	0.03	0.04	0.13	0.72
9	13.83	-0.07	0.62	0.01	0.03	0.19	0.55
10	15.14	-0.29	0.57	0.00	0.03	0.18	0.55
11	19.09	-1.68	0.45	0.20	0.18	0.08	0.77
12	20.94	-3.27	0.43	0.22	0.19	0.05	0.81
13	20.94	-2.74	0.43	0.13	0.19	-0.02	0.78
14	23.25	-3.53	0.38	0.22	0.20	0.01	0.82
15	23.29	-3.30	0.41	0.11	0.20	-0.01	0.79
16	23.29	-1.75	0.41	0.10	0.20	-0.03	0.85
17	22.90	-3.69	0.40	0.14	0.19	0.00	0.78
18	23.33	-2.49	0.41	0.04	0.21	-0.08	0.68
19	23.33	-2.31	0.41	0.02	0.21	-0.08	0.77
20	24.49	-2.06	0.40	0.04	0.18	-0.03	0.81
21	24.95	-1.34	0.33	0.17	0.11	0.07	0.80
22	24.53	-0.93	0.34	0.21	0.10	0.08	0.78
23	24.53	1.26	0.34	0.09	0.10	0.07	0.73
24	25.34	-0.88	0.35	0.14	0.12	0.04	0.77
25	25.34	-0.34	0.35	0.13	0.12	0.04	0.85
26	26.25	-0.45	0.36	0.08	0.13	0.05	0.68

603

604 Table SOM-2 Statistics of the time series of the localized SST-analysis (LA-ERSST) data series at the 26
605 station, as well as the differences (Diff) between the pairs of time series. The correlation coefficients
606 between LH and LA-ERISST are also calculated (the 90% confidence level is 0.22, without considering
607 serial correlation). Red numbers indicate that the correlation coefficients do not exceed the 90% confidence
608 level.

No	Mean LA-ERSST	Diff	Std-dev LA-ERSST	Diff	Trend (°C/10yrs)	Diff	Corr
1	12.26	-0.76	0.53	0.00	0.16	0.01	0.69
2	12.06	0.15	0.55	0.03	0.17	0.09	0.70
3	12.68	-1.14	0.54	0.17	0.17	0.12	0.82
4	13.59	-2.23	0.52	0.07	0.16	0.05	0.78
5	12.65	0.71	0.54	0.05	0.16	0.06	0.77
6	13.16	-0.51	0.52	0.06	0.16	0.01	0.79
7	14.62	-2.53	0.50	0.09	0.14	0.00	0.76
8	14.62	-0.25	0.50	0.14	0.14	0.03	0.85
9	14.62	-0.86	0.50	0.12	0.14	0.08	0.78
10	15.92	-1.06	0.50	0.07	0.12	0.09	0.81
11	18.68	-1.27	0.46	0.19	0.10	0.16	0.65
12	21.18	-3.51	0.37	0.28	0.12	0.12	0.70
13	21.18	-2.98	0.37	0.19	0.12	0.05	0.71
14	24.37	-4.39	0.32	0.20	0.12	0.09	0.69
15	24.37	-2.83	0.32	0.19	0.11	0.08	0.75
16	23.02	-3.80	0.33	0.22	0.11	0.06	0.77
17	23.02	-3.30	0.33	0.28	0.12	0.07	0.71
18	24.37	-3.53	0.32	0.13	0.11	0.02	0.63
19	24.37	-3.35	0.32	0.12	0.11	0.02	0.65
20	25.44	-3.01	0.31	0.13	0.09	0.06	0.67
21	25.28	-1.66	0.35	0.14	0.04	0.14	0.56
22	25.23	-1.63	0.41	0.15	0.02	0.18	0.49
23	25.23	0.56	0.41	0.03	0.03	0.17	0.37
24	25.81	-1.35	0.37	0.12	0.01	0.16	0.54
25	25.81	-0.81	0.37	0.11	0.01	0.16	0.66
26	25.96	-0.16	0.34	0.10	0.05	0.13	0.47

609

610